

Comparison on the traveling wave excitation and the conventional excitation

B. ZHANG¹, D. K. Sodickson¹, R. Lattanzi¹, Q. DUAN¹, R. Brown¹, B. Stoeckel², and G. Wiggins¹

¹CBI, Department of Radiology, New York University, NEW YORK, NY, United States, ²Siemens Healthcare

Introduction: Traveling wave imaging has been suggested as a promising method for large FOV imaging in high field MR because in the empty bore it has a nearly constant magnitude along the propagating direction. However, the traveling wave system has thus far not been quantitatively compared with the conventional volume coil designs at high field to evaluate its performance in terms of efficiency, homogeneity and SAR for whole body imaging. In this work, we use the finite difference time domain (FDTD) method to simulate a stepped-diameter traveling wave system and TEM resonator system loaded with the same body model, and compare the simulation results of these two systems in terms of B1 mapping, SAR distribution and system efficiency.

Methods: The actual configuration in 7 Tesla MR system is a stepped-diameter waveguide formed by the conductive surfaces of the cryostats, gradient coil and RF shield. This is modeled in CST by constructing a cylindrical conductive shield representing the cryostat, (900mm in diameter, 3360mm in length), narrowing at the RF shield (680mm diameter, 1220mm in length) in the center. A patch antenna with two orthogonal coax feeds matched to 50Ohm was modeled for excitation and reception at 7T [2]. Following a design presented by Vaughan et.al [3], a TEM resonator is modeled with an inner diameter of 58cm and an RF shield of 62 cm. We also model this as a stepped diameter system, with the 122cm length of 62cm RF shield positioned in the middle of a 90cm diameter warm bore to match the conditions in an actual scanner. The TEM coil consists of 24 rods evenly placed around the cylinder with their centers on a circle of 58.3cm diameter, rung diameters of 0.6cm and its rung lengths of 33cm. Four driving ports are placed at 90-degree intervals around the rungs. Since the body model intersects with one rung when it is placed in the center of the TEM body coil, the body model was raised up by 3.8cm to avoid it touching the rungs. An additional simulation was run with a body model with the arms excluded. In order to match the driving ports to 50ohm, a pi circuit network was used. It should be noted that since four driving ports are used in the TEM body coil while only two driving ports are used in the traveling wave system, the voltage at each port is scaled so that the same total power is sent to each system. These two systems are tuned and matched in the empty bore and re-tuned and re-matched when it is loaded with the body model. B1 mapping and SAR distribution of both systems with/without body are compared.

Results: Figure 1 shows axial B₁⁺ maps on a dB scale of the empty traveling wave system (TWS) and TEM system. In an axial plane at isocenter, the TWS creates a B₁⁺ field which is peaked at the center and diminishes towards the edge of the bore. This drop-off towards the edge of the bore can be attributed to the nature of the TE₁₁ mode in which the B field is oriented primarily along Z near the shield. In contrast, the B₁⁺ field produced by the TEM in an axial slice has strong peaks near the rungs, but is nearly flat (+/- 0.1dB over a central circle of 46cm diameter). The B₁⁺ magnitude at isocenter is 5.6dB higher for the TEM compared to the TWS. Looking at the coronal B₁⁺ maps (Fig. 2) we see that the TWS creates a B₁⁺ field which fills the bore. A profile along Z down the center of the bore varies by only 1dB along the length of the gradient RF shield. For the TEM, as expected, and in contrast to the traveling wave system, the B₁⁺ field drops off outside of the active volume of the TEM coil. Within the volume defined by the active elements the B₁⁺ field varies by 3dB, and at the end of the TEM shield the B₁⁺ field has dropped by approximately 7dB. Although the B₁⁺ field in the empty waveguide is quite uniform in the traveling wave system, the wave behavior with the body model present is quite complicated. The E field and B field patterns in the free space between the body model and the patch antenna are almost the same as those in the empty bore. However, as soon as the traveling wave interacts with the body, there is an evident attenuation, and complicated wave behavior in the body is observed [3]. With TEM excitation, the B₁⁺ pattern produced in the body is also complex and inhomogeneous, with significant signal voids due to destructive interference [5]. Animations of the H field vectors (not shown) reveal that the TEM creates some degree of traveling wave excitation outside the volume of the active elements. For the empty bore the traveling wave excitation is approximately 18% of the standing wave excitation at isocenter. This traveling wave excitation presumably contributes to the significant excitation seen in the head and legs with the TEM coil. Figure 2 shows B₁⁺ maps for the TWS and TEM systems when the subject is head first towards the patch antenna. With the TWS, the highest B₁⁺ field occurs in the brain stem. The signal at the surface of the body is strong, but decays very quickly as it goes deeper into the torso. Correspondingly, for the TEM system, it can be seen that the strongest B₁⁺ field is in the arms and weakest signal in deep torso. The high degree of inhomogeneity in both systems makes quantitative comparison difficult. One useful metric is to calculate the average B₁⁺ field across an axial slice through the heart for the two systems. For the TWS the average B₁⁺ is 0.079, compared to 0.2449 for the TEM. Thus on average the TEM produces 3 times stronger B₁⁺ in an axial slice through the torso at the center of the coil. The result is approximately the same if we remove the arms from the body model, which clearly interact strongly with the TEM elements. The SAR distribution for the two systems is shown in Figure 4. The stimulated power for the TWS is 1W (root mean square) and the absorbed power is 0.76, thus the system efficiency is 76%. The total SAR is 0.0066 W/kg and the maximum point SAR is 0.23W/kg which is located at the brain stem. From Figure 4, it can be seen that TWS SAR is highest in head and arms, still high in the surface area of the body and also in the legs, while becomes low in deep torso and spine. For the TEM the stimulated power (root mean square) is 1W and the absorbed power is 0.922, thus the system efficiency is 92.2%. The total SAR is 0.0156W/kg and the maximum point SAR is 5.33W/kg which is located in the arm. Since the arms are quite close to the rungs this creates a strong SAR hotspot. If we remove the arms from the body model (as though the subject had raised their arms up over their head and out of the TEM coil) the peak local SAR for the TEM is reduced to 0.37W/kg. Considering that the average B₁⁺ is 3 times higher with the TEM we could achieve the same excitation with 9 times less power, bringing the SAR limit of the TEM into 0.6W/kg comparison with the TWS. It should also be pointed out that it is possible with a decoupled multi-element TEM coil to perform B1 shimming and accelerated parallel transmit to mitigate the strong inhomogeneities in the body [5], something which is not possible with a 2 channel patch antenna excitation.

Conclusions

The traveling wave system and conventional TEM body coil in 7T are simulated to compare in terms of B1 mapping, SAR distribution and system efficiency. Both systems show strong B₁⁺ inhomogeneities in the torso, though these could in principle be mitigated with a parallel multi-port TEM excitation. The combination of strong attenuation of the traveling wave and high SAR in tissues near the patch antenna make the TWS less suitable for whole body imaging than a local standing wave transmitter such as the TEM.

References

[1] D.O. Brunner et al. 16th ISMRM, Toronto 2008. [2] B. Zhang et al, ISMRM 2009, P.4746 [3]. C.A. van den Berg, et al. ISMRM 2009. [4] B. Zhang et al, ISMRM 2009, P498. [5] C.A. van den Berg, et al. MRM 2009.

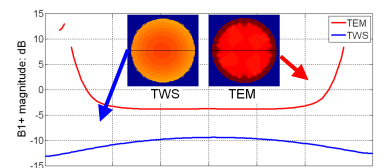


Figure 1: Axial B₁⁺ maps and profiles for the TWS and TEM systems, on a dB scale

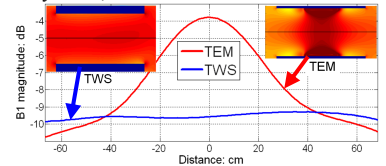


Figure 2: Coronal B₁⁺ maps and profiles for the TWS and TEM systems

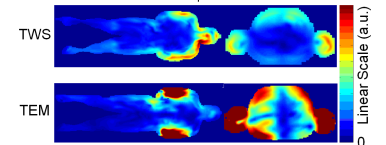


Figure 3: B₁⁺ maps with a body for the TWS and TEM systems (Linear scale)

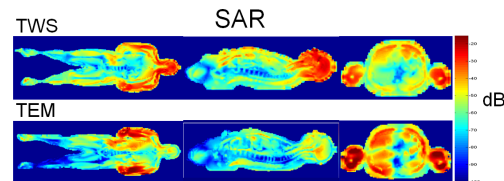


Figure 4: SAR maps with a body for the TWS and TEM systems (Linear scale)